Received: 14 January 2020 | Revised: 25 May 2020 | Accepted: 18 June 2020

DOI: 10.1111/mec.15535

ORIGINAL ARTICLE

MOLECULAR ECOLOGY WILEY

Meta-analysis of the coral environmental stress response: *Acropora* corals show opposing responses depending on stress intensity

Groves Dixon | Evelyn Abbott | Mikhail Matz

Department of Integrative Biology, University of Texas, Austin, TX, USA

Correspondence
Groves Dixon, Department of Integrative Biology, University of Texas, Austin, TX, USA
Email: grovesdixon@gmail.com

Funding information
National Science Foundation, Grant/Award Number: IOS-1755277

Abstract

As climate change progresses, reef-building corals must contend more often with suboptimal conditions, motivating a need to understand coral stress response. Here, we test the hypothesis that there is a stereotyped transcriptional response that corals enact under all stressful conditions, functionally characterized by downregulation of growth, and activation of cell death, response to reactive oxygen species, immunity, and protein folding and degradation. We analyse RNA-seq and Tag-Seq data from 14 previously published studies and supplement them with four new experiments involving different stressors, totaling over 600 gene expression profiles from the genus *Acropora*. Contrary to expectations, we found not one, but two distinct types of response. The type A response was observed under all kinds of high-intensity stress, was correlated between independent projects and was functionally consistent with the hypothesized stereotyped response. The consistent correlation between projects, irrespective of stress type, supports the type A response as the general coral environmental stress response (ESR), a blanket solution to severely stressful conditions. The distinct type B response was observed under lower intensity stress and was more variable among studies. Unexpectedly, at the level of individual genes and functional categories, the type B response was broadly opposite the type A response. Finally, taking advantage of the breadth of the data set, we present contextual annotations for previously unannotated genes based on consistent stress-induced differences across independent projects.

KEYWORDS
coral, gene regulation, general stress response, reef, RNA-seq, transcriptomics

1 | INTRODUCTION

Coral reefs provide disproportionately high ecological and socioeconomic benefits but are among the ecosystems most threatened by climate change. This has motivated efforts to understand mechanisms of coral resilience to environmental stress. A popular method for approaching such questions is profiling genome-wide gene expression using RNA-seq (Drury, 2019). Often, these studies focus on a single stressor and seek to identify genes and pathways that underlie the adaptive responses to it. However, in isolation, these studies cannot differentiate between gene regulation specific to a particular stressor, and gene expression changes reflecting stress in general. For this reason, delineation of corals' general stress response is needed to understand how they contend with suboptimal conditions.

The concept of a generalized stress response has been investigated thoroughly in prokaryotes. Here, the general stress response

refers to a set of genes coordinately induced under diverse stressful conditions by the activity of alternative sigma factors, which competitively bind with RNA polymerase to transcribe particular genes (Ron, 2006). Inducing conditions include starvation, acid stress, osmotic shock, and temperature shock among others. In *E. coli*, the general stress response is driven by alternative sigma factor σS, which directly or indirectly regulates up to 10% of the genome (Weber et al., 2005). The *E. coli* heat shock response is similarly regulated by alternative sigma factors σ^{32} and σ^{E} (Ron, 2006). In the gram-positive bacterium *B. subtilis*, many of the heat shock proteins are regulated as part of the general stress response controlled by alternative sigma factor σ^{B} (Ron, 2006).

General stress responses have also been described in eukaryotes. For instance, the transcription factor p53 has been described as a general stress response gene (Young, Locke, & Elowitz, 2013), as it is activated not only by DNA damage, but also by hypoxia, oxidative stress, protein damage, and heavy metal toxicity (Abdulla & Campbell, 1996; Hammond & Giaccia, 2005). In *Sacharomyces cerevisiae*, Gasch et al. (2000) identified a stereotyped pattern of gene expression induced by diverse environmental stressors including temperature shock, nutrient limitation, oxidative stress, and osmotic shock, which they referred to as the environmental stress response (ESR). The ESR was characterized by downregulation of growth-related processes, and upregulation of carbohydrate metabolism, detoxification, cell wall modification, protein folding and degradation, DNA damage repair, fatty acid metabolism, metabolite transport, vacuolar and mitochondrial functions, autophagy, and intracellular signaling. They proposed that this stereotyped expression pattern is a blanket adaptive response to suboptimal conditions (Gasch et al., 2000).

A transcriptional response resembling the ESR in yeast appears to exist in Cnidarians. Examining functional enrichment among heat stress genes in *Acropora hyacinthus* and other coral studies, Barshis et al. (2013) pointed out conspicuous similarity to the yeast ESR (Gasch et al., 2000; Brion et al., 2016). Comparing heat stress responses among anemone strains, Cziesielski, Schmidt-Roach and Aranda (2019) describe a "core Cnidarian response to heat stress" including protein folding and oxidative stress genes. The idea of a general stress response was also described by Aguilar et al. (2019). Examining results from multiple RNA-seq studies, they point out complements of genes, including oxidative stress genes and heat shock proteins (HSPs), that are consistently differentially expressed under environmental stress. Indeed, there is a key set of gene functions mentioned in most gene expression studies on coral stress. These include downregulation of growth-related processes, and upregulation of protein folding and degradation, oxidative stress response, immune response, and cell death (DeSalvo, Estrada, Sunagawa, & Medina, 2012; Kenkel, Meyer, & Matz, 2013; Kenkel, Moya, Strahl, Humphrey, & Bay, 2018; Maor-Landaw et al., 2014; Meyer, Aglyamova, & Matz, 2011; Table 1). Hence the existence of a general coral stress response has been widely hypothesized but has yet to be comprehensively tested across diverse environmental stressors.

Here, we test the hypothesis of the general ESR in reef-building corals by collectively reanalysing publicly available RNA-seq data sets conducted on the coral genus *Acropora*, along with four new experiments. The use of the same pipeline and reference genome for all data sets makes them directly comparable. Specifically, we test whether there exists a core transcriptional response that corals enact under widely different forms of environmental stress (a coral ESR). This general stress response can be contrasted with specific responses that are induced only by particular stressors. The existence of a general ESR makes several predictions about coral gene expression under diverse stressful conditions: (a) gene expression responses to different stressors should be similar. If we measure $\log_2$ fold changes in gene expression between stress-treated and control samples, these changes should correlate between independent studies applying distinct stressors, reflecting the general nature of the response; (b) gene expression responses to diverse stressors should demonstrate shared enrichment for the functions above; and (c) it should be possible to identify sets of coregulated genes up- and downregulated by all types of stress.

2 | MATERIALS AND METHODS

2.1 | Data sources

Relevant studies were identified by searching for the genus name *Acropora* on the NCBI SRA database. Only studies with Illumina data were used, giving 36 in total (Table 1). To make the data sets fully comparable, we obtained raw sequencing reads and mapped them all to the same reference, the recently assembled high-quality genome of *Acropora millepora* (Fuller et al., 2019). Our initial exploration (Figure 1) included the entire set of 36 studies. Only a subset of 15 of these studies included a stress treatment (Table 1). Analyses of the coral ESR included only these 15 studies. A summary of the treatments applied in these studies is shown in Table S2. These 'stress' studies were identified based on descriptions of the treatments in the SRA metadata, and the studies' manuscripts. The remaining studies compared gene expression between treatments none of which would be obviously stressful, such as differences due to lunar cycle, or developmental timepoint under ambient condition. While some ecological sites are considered higher quality than others, we not did consider ecological sample site as a basis for stress treatment.

A copy of the SRA metadata Table used for the BioProjects used in this study is shown in Table S2. Whenever possible, sample traits were filled in from information included in the SRA metadata Table. When not possible, sample information was obtained from the BioSample accessions, publications, and in a few cases, by directly asking the authors. The final modified version of the sample trait table used for analysis is given as Table S3.

The analysis also included RNA-seq reads from four new experiments in our laboratory. These experiments were conducted at Orpheus Island Research Station in November 2018, under

TABLE 1 BioProjects included in study

BioProject	Reference	Year	Stress study	Species
PRJNA149513	Moya et al. (2012)	2012	Yes	*millepora*
PRJNA177515	Barshis et al. (2013)	2013	Yes	*hyacinthus*
PRJNA222758	Libro et al. (2013)	2013	Yes	*cervicornis*
PRJNA200542	Weiss et al. (2013)	2013	Yes	*millepora*
PRJNA242821	Palumbi, Barshis, Traylor-Knowles, Bay (2014)	2014	No	*hyacinthus*
PRJNA266455	Rosic et al. (2014)	2014	Yes	*aspera*
PRJNA288809	Bertucci, Forêt, Ball, Miller (2015)	2015	No	*millepora*
PRJNA279192	Dixon et al. (2015)	2015	Yes	*millepora*
PRJNA276913	Kaniewska, Alon, Karako-Lampert, Hoegh-Guldberg, Levy (2015)	2015	No	*millepora*
PRJNA269992	Kaniewska et al., 2015)	2015	Yes	*millepora*
PRJNA260269	Moya et al. (2015)	2015	Yes	*millepora*
PRJNA274410	Seneca & Palumbi (2015)	2015	Yes	*hyacinthus*
PRJNA309168	Mohamed et al. (2016)	2016	No	*digitifera*
PRJDB3244	Reyes-Bermudez, Villar-Briones, Ramirez-Portilla, Hidaka, Mikheyev (2016)	2016	No	*digitifera*
PRJNA292574	Strader, Aglyamova, Matz (2016)	2016	No	*millepora*
PRJDB4562	Takahashi-Kariyazono, Gojobori, Satta, Sakai, Terai (2016)	2016	No	*digitifera,tenuis*
PRJDB4579	Yasuoka, Shinzato, Satoh (2016)	2016	No	*digitifera*
PRJNA380267	Aguilar et al. (2017)	2017	Yes	*millepora*
PRJNA411943	Bay, Rose, Logan, Palumbi (2017)	2017	No	*hyacinthus*
PRJNA298496	Gajigan & Conaco (2017)	2017	Yes	*digitifera*
PRJNA316795	Rosenberg, Doniger, Harii, Sinniger, Levy (2017)	2017	No	*digitifera*
PRJNA338455	Ruiz-Jones & Palumbi (2017)	2017	No	*hyacinthus*
PRJNA319662	Wright et al., 2017)	2017	Yes	*millepora*
PRJNA308355	Zhou et al. (2017)	2017	Yes	*aculeus*
PRJNA362652	Kenkel et al., 2018)	2018	No	*millepora*
PRJNA398338	Mohamed et al. (2018)	2018	No	*digitifera*
PRJNA293100	Oldach & Vize (2018)	2018	No	*gemmifera*
PRJNA423227	Parkinson et al. (2018)	2018	Yes	*cervicornis*
PRJNA379450	Rose, Bay, Morikawa, Palumbi (2018)	2018	No	*hyacinthus*
PRJNA379147	Strader, Aglyamova, Matz (2018)	2018	No	*millepora*
PRJDB6468	Takahashi-Kariyazono, Sakai, Terai (2018)	2018	No	*digitifera*
PRJNA380146	Yuan et al. (2018)	2018	No	*gemmifera*
PRJNA476311	Rocker, Kenkel, Francis, Willis, Bay (2019)	2019	No	*tenuis*
PRJNA386795	None	2017	No	*palmata*
PRJDB4715	None	2018	No	*tenuis*
PRJNA559404	(this study)	2020	Yes	*millepora*

GBRMPA permit G18/41245.1. Four adult colonies of *A. millepora* were collected by SCUBA: three from Northeast Orpheus (labelled N1, N2, and N10), and one from Little Pioneer Bay (labelled L1), and transported back to raceways of unfiltered seawater. Nubbins were broken off from the colonies and maintained in the raceway on dish racks for 10–17 days before experiments were conducted. Treatments were intended to cause bleaching by acute stress, and are described in the following sections.

2.2 | Cold stress

The cold stress experiment included a cold and a control treatment group. Each treatment group comprised three replicate "twigs" (small branches with 2–3 tips) from each of the four colonies (genets; $N = 12$ twigs per treatment group). Treatments were conducted by hanging twigs in 10 L containers using fishing line (1 container per treatment; 12 nubbins per container). The cold treatment group

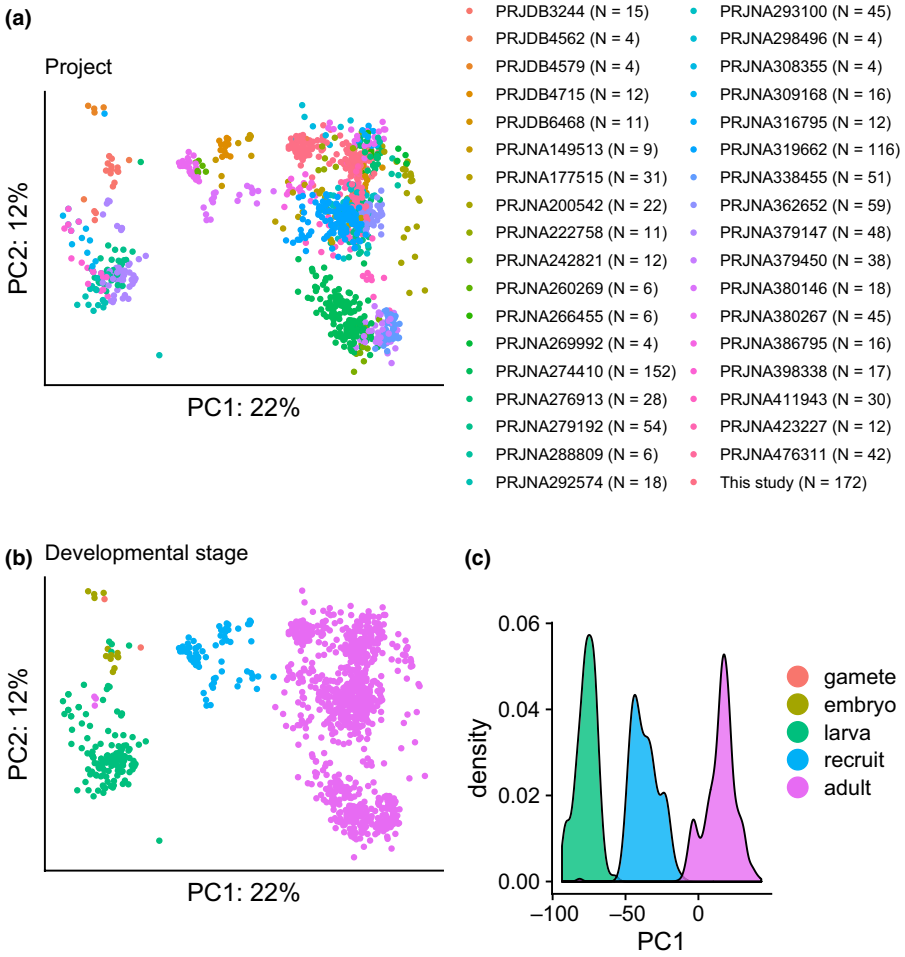

FIGURE 1 Principal component analysis (PCA) of the full data set. PCA was conducted on normalized read counts for the top 10% most variable genes, after accounting for differences due to varying read counter for each sample (see methods). (a) PCA colour coded by BioProject (the source of the published reads; 36 total projects). The legend shows the BioProject accessions along with the number of samples included in each. (b) The same PCA colour coded by developmental stage. (c) Density plot of PC1 for three primary developmental stages [Colour figure can be viewed at wileyonlinelibrary.com]

container was placed in a refrigerator at 4°C for 6 hr, after which it was returned to ambient temperature. This treatment produced a ramp downward to 10.6°C over 6 hr followed by a ramp back to ambient temperature over another 6 hr (Figure S1). At the same time, the control group container was moved into a cabinet to mimic the dark of the cold treatment. Tissue samples (one branch per twig) were fixed in ethanol 17 hr after initiation of the 4°C treatment and immediately stored at −80°C. At this time point, the corals showed visible signs of bleaching (Figure S1).

2.3 | Hyposalinity stress

The hyposalinity stress experiment included a hyposalinity and a control treatment group. Each treatment group comprised three replicate twigs from each of the four colonies ($N = 12$ nubbins per treatment group). Here each treatment was applied in three replicate 5 L containers, each containing a single twig from the four colonies (three containers per treatment; 4 twigs per container). The three control containers were filled with filtered seawater. The three hyposalinity containers were filled with 42.8% filtered seawater (~15 ppt) by mixing 2.14 L of seawater with 2.86 L freshwater. We chose this treatment instead of less severe hyposalinity treatments because it caused bleaching in 100% of samples in trial experiments. Corals were moved directly into hyposalinity or control conditions from the raceway, and held with air circulation for 6 hr, after which flow of filtered seawater was resumed. Samples were fixed in ethanol 6 hr after beginning the exposure (immediately before resuming seawater flow). These samples already showed visible signs of bleaching. An additional set of samples was fixed 14 hr after beginning the exposure (8 hr after seawater flow was resumed). Samples were stored at −80°C immediately after fixing. A schematic of the experiment and example photos of control and treated samples are shown in (Figure S2).

2.4 | Heat stress

The heat experiment included a heated and control treatment group, each with three replicate twigs from each of the four colonies ($N = 12$ nubbins per treatment group). Treatments were applied in single 10 L containers. The single heated container was ramped to 36°C over 3 hr and held at 36°C for three additional hours by drip flow of 36°C filtered seawater in a room with air temperature set to 36°C. We then returned the container to a shaded table outside, allowing it to ramp back to 28°C over 3 hr. The control container was kept in a similar room at ambient temperature (~28°C) with similar flow of (~28°C) filtered seawater and returned to the shaded table at

the same time. We chose the heat treatment temperature to ensure bleaching in 100% of samples based on trial experiments using 34°C, 35°C and 36°C. Samples were fixed in ethanol 14 hr after the treatment was started (5 hr after the returning to ambient temperature). Samples showed visible signs of bleaching at this point. For one of the colonies (N1), all three replicates had died by the sampling point. A second set of tissue samples was fixed in ethanol 25 hr after treatment was started. Samples were stored at −80°C immediately after fixing. Temperature traces for the experiment and example photos of control and treated samples are shown in (Figure S3).

2.5 | Multistress treatment

A final experiment was conducted with four treatment groups. These included a control group, a second heat treatment group, and two groups with multiple stressors. The heat treatment group was ramped to 35°C over 3 hr and held for three additional hours before ramping back down to ambient temperature (~28°C) over 2 hr (Figure S4) using drip flow and a heated room as described for the previous heat experiment. The multi-stress groups were exposed to a combination of hot and then cold temperature or cold and then hot temperature simultaneously with mild hyposalinity (71.4% filtered seawater; ~25 ppt). The hot-then-cold treatment group was ramped to 35°C over 3 hr, and then moved to a refrigerator at 4°C for 3 hr, which dropped the temperature to a low point of 24.2°C, then returned to an outdoor tabletop, where the temperature returned to 28°C over 3 hr (Figure S5). The cold-then-hot treatment group received the reverse; first placed in the refrigerator at 4°C for 3 hr, reducing the temperature to a low point of 19.4°C, then ramping to 35°C over 3 hr before it was moved to an outdoor tabletop allowing a return to ambient temperature over 3 hr (Figure S5). Tissue samples were fixed in ethanol 13 and 23 hr after the experiment began. Flow of filtered seawater was resumed after the first set of samples was fixed. By mistake, flow was not returned to the hot-then-cold treatment group. For this reason, this group was not fixed at the second time point. At 7.5 hr after the experiment began an additional set of tissue samples was fixed from a single colony (N10) because they appeared to be dying in the multistress treatment groups. These were taken in addition to the other tissue fixing time points.

2.6 | Library preparation

RNA was isolated using RNAqueous Total RNA Isolation Kits. Coral tissue was submerged in lysis buffer and pulverized using a single 6 mm diameter chrome steel bead (Biospec Cat No. 11079635c) and a Biospec Mini-Beadbeater-96 (Cat. No. 1,001) using 20 s beating duration. The resulting lysate was processed according to the RNAqueous protocol. Preparation of tag-seq libraries (Dixon, Bay, & Matz, 2014, 2016; Kenkel & Matz, 2016; Meyer et al., 2011) was carried out at the Genome Sequencing and Analysis Facility at The University of Texas Austin. Single-end sequencing of 50 bp length reads was done on a single lane of an Illumina HiSeq 2,500 (172 samples per lane).

2.7 | Sequence data processing

Detailed steps for the data processing pipeline, along with all custom scripts used during data processing are archived with ZENODO (https://doi.org/10.5281/zenodo.3902307) and maintained on GITHUB: https://github.com/grovesdixon/Acropora_gene_expression_meta.git. Fastq files for each previously published sequencing run were downloaded using the SRA toolkit. Adapter trimming was performed in paired- or single-end mode as appropriate for each study using cutadapt (Martin, 2011), with a minimum length cutoff of 20 bp and a PHRED quality cutoff set to 20. Quality of reads was assessed before and after trimming on a subset of 10,000 reads from each Run using FASTQC (Andrews, 2010). Reads were mapped to an annotated draft reference genome for *Acorpora millepora* (Fuller et al., 2019). The reference genome was generated using a combination of PacBio reads and Illumina paired-end reads with 10X Chromium barcodes and anchored into chromosomes with linkage mapping data from two previous studies (Dixon et al., 2015; Wang et al. 2009). Mapping was performed with BOWTIE2 in paired- or single-end mode as appropriate using the --local argument, otherwise using default parameters (Langmead & Salzberg, 2012). Following alignment, PCR duplicates were removed using MarkDuplicates from Picard Toolkit (Broad Institute, 2019). Sorting and conversion from sam files was performed using Samtools (Li et al., 2009). The reads mapping to annotated gene boundaries were counted using FeatureCounts (Liao, Smyth, & Shi, 2014). Mean absolute and relative read counts for each BioProject throughout the processing pipeline are shown in (Figure S6) and total read counts for individual samples in (Table S4). As visible in Figure S6, there was substantial variation between BioProjects in both the absolute number of reads produced and the mapping efficiencies. As the BioProjects included nine different species of *Acropora* (Table S1; Table S2), and were all mapped to the *A. millepora* reference genome, we examined whether species was a significant factor in determining mapping efficiency or the final number of counted reads. Using analysis of variance, we found that on its own, species explained 21.5% of variance in mapping efficiency. However, when we accounted for variance due to BioProject (59.6% of variance explained), the percentage for species was reduced to a nonsignificant 0.03%. Final gene counts were even more strongly dependent on BioProject. Here, after accounting for BioProject (95.1% of variance explained), species accounted for <0.01% of variance. Hence, despite mapping all species to the same reference, BioProject appeared to be a much more important factor than species in predicting the mapping efficiency and final fold coverage.

2.8 | Principal component analysis

We used principal component analysis (PCA) to summarize transcriptional variation for two data sets. The first, shown in Figure 1,

was the full data set, which included all 36 BioProjects found on the SRA database (Table 1; Table S2). The second data set (shown in Figure 2) included only the 15 BioProjects that applied a stress treatment (Table 1). Our exploration of the full data set served primarily as a quality check to ensure we could identify the expected variation in transcription between developmental stages before continuing to our analyses of stress response. In both cases, raw read counts were normalized using the vst() function in the R package DESeq2 (Love, Huber, & Anders, 2014), and the top 10% of genes with the greatest variance was used as input. Hence, the input for PCA was an m x n matrix, with m rows = total number of sample individuals and n columns = 1/10th of the total number of genes, with entry a_{ij} indicating the mRNA abundance (on a variance-stabilized log scale) of gene j in sample i. PCA was performed on this input using the prcomp() function in R. In our first iteration of the analysis using the full data set, the first principal component correlated closely with raw read counts ($R^2 = 0.61$). This apparent contribution of sequencing effort to overall variation was surprising and indicated that in this case, the vst() function had not removed all variance associated with total raw read count. Based on this, we used the removeBatchEffect() function in R package LIMMA (Ritchie et al., 2015) to control for the total number of reads counted on genes by FEATURECOUNTS then performed PCA again. Scores from the resulting PCA (Figure 1) were assessed visually for clustering of samples based on BioProject (the original study the sequencing run came from), treatment, and developmental stage of the sample (gamete, embryo, larva, or adult). Here, the first principal component was found to correlate closely with developmental stage. Controlling for BioProject using limma::removeBatchEffect removed the correlation between PC1 and developmental stage observed in Figure 1, ostensibly because each project typically had samples of

(a)

Treatment	N projects	N samples	N bleached
control	15	283	0
heat	8	143	121
cold	2	16	12
hyposalinity	2	42	20
immune challenge	3	91	0
low pH	2	9	0
multiple	2	34	34

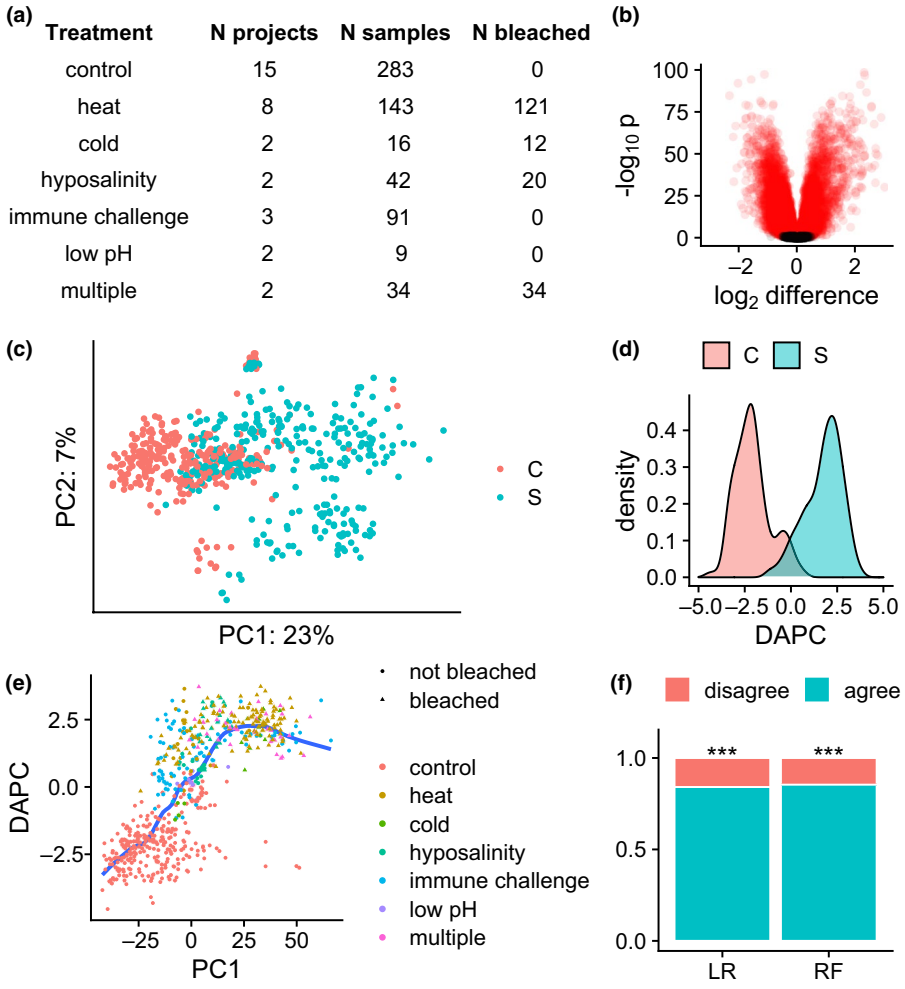

FIGURE 2 Transcriptional response to stress treatments. (a) Table showing the number of projects and samples for each type of stress. (b) Volcano plot showing $\log_2$ fold differences and p-values for difference between all stressed and control samples. Positive $\log_2$ fold differences indicate upregulation in stressed samples. Red points indicate significant genes (FDR < 0.05). (c) Principal component analysis (PCA) of samples from all projects that included a stress treatment. (d) Density plot of sample loading values for discriminant analysis of principal components (DAPC) performed to discriminate stressed and control samples. (e) Scatterplot of PC1 and DAPC loading values. Point colour indicates the type of stress applied. Point shape indicates whether the study reported bleaching among stressed samples. (f) Barplot of accuracy percentages when predicting stressed status based on gene expression using logistic regression (LR) and random forest models (RF). Models were trained on a random subset of 60% of the samples stratified by BioProject and accuracy was measured based on predictions made for the remaining 40% of samples [Colour figure can be viewed at wileyonlinelibrary.com]

just one life cycle stage, and nonadult samples were relatively rare. In other words, because larval and recruit samples were limited to only a few BioProjects, controlling for variation due to BioProject removed most of the variation from developmental stage as well. For this reason, the PCA of the full data set (Figure 1) was generated without controlling for BioProject.

We next used PCA to explore variation only among BioProjects that applied a stress treatment (Stress study = yes in Table 1). Among these studies, only one (Dixon et al., 2015) used samples from more than one developmental stage (adults and larvae). The only other studies to use nonadult samples were Moya et al. (2012) and Moya et al. (2014), which used recruits. To simplify downstream analyses, only the adult samples from Dixon et al., 2015 were retained. In an initial PCA of this data set, we again found a strong influence of BioProject, but less so for raw read counts compared to the full data set. Hence, to build the PCA shown in Figure 2, we first subset the full raw counts matrix for the 15 BioProjects that applied stress treatments, then normalized the matrix using vst(), then controlled for BioProject using limma::removeBatchEffect, subset for the top 10% most variable genes, then applied prcomp() function.

2.9 | Differential gene expression analysis

To identify genes differentially expressed in response to different stress treatments, we used DESeq2 (Love et al., 2014). A total of 15 projects were found to include stress treatment (Figure 2a). For all differential expression analyses, stress treatment was encoded as a binary variable, either "stress" or "control". For studies that applied a range of stress treatments, intermediate stress treatments were coded as "stress". For instance, if a project exposed corals to 350, 750, and 1,000 ppt CO_2, and 350 ppt was the control condition, then both 750 ppt and 1,000 ppt samples were coded identically as 'stress'. To compute $\log_2$ fold differences due to stress across all stress studies (Figure 2b) we used both stress treatment and BioProject as predictive variables, then reported $\log_2$ fold differences for the stress versus control contrast. We also performed differential expression analysis for each BioProject individually. For each data set, genes with mean read count less than three were removed before differential expression analysis. This relatively low cutoff was chosen to eliminate extremely low coverage genes before initiating differential expression analysis. The value three was chosen to include as many genes as possible while eliminating genes with too little fold coverage for differential expression analysis. Significance of stress

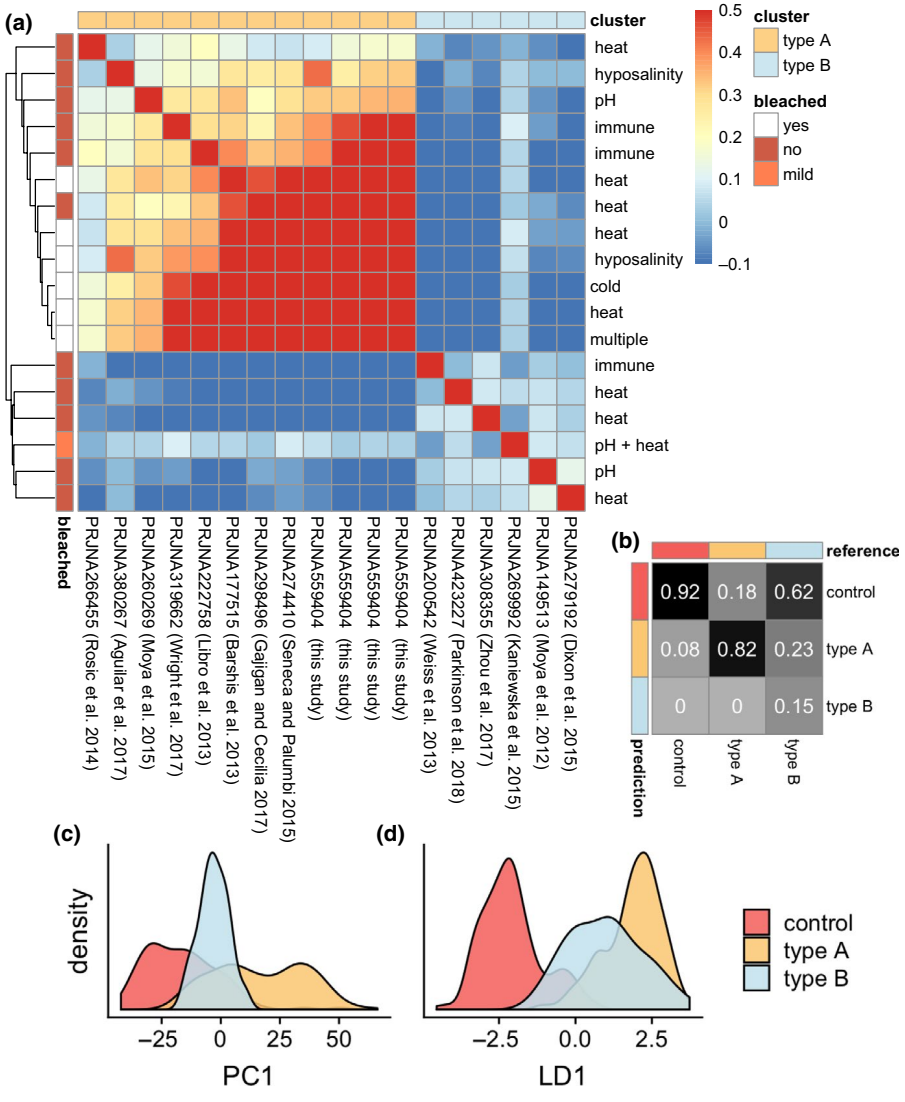

FIGURE 3 Identification of two types of stress response. (a) Heatmap of correlations of stress-induced gene expression between BioProjects. Column labels indicate the BioProject and reference. Row labels indicate the type of stress treatment. Data sets were hierarchically clustered based on correlation. Cell shading indicates Pearson correlation of the $\log_2$ fold differences due to stress treatment for all genes between the indicates BioProjects. Columns are annotated with shading based on inferred cluster assignment (type A or B). Rows are annotated with shading based on reported bleaching among stress-treated samples. (b) Confusion matrix showing holdout prediction frequencies for the random forest validation set. Columns indicate the reference state, rows indicate the prediction. For example, cells along the diagonal indicate correct predictions, whereas 62% type B stressed samples were misidentified as controls. (c) Density plot for control, cluster A stressed, and cluster B stressed samples along PC1 from Figure 2c. (d) Density plot for same samples along the DAPC axis from Figure 2d [Colour figure can be viewed at wileyonlinelibrary.com]

treatment was tested using Wald tests. This is the default method for significance testing in DESeq2, and has the computational advantage over likelihood ratio tests because it does not require fitting a pair of full and reduced models. When comparing gene expression responses between BioProjects (Figure 3a), we report the Pearson correlation of $\log_2$ fold differences for each pair of BioProjects computed from all expressed genes (mean fold coverage > 3 in both BioProjects).

2.9.1 | Discriminant analysis of principal components

Discriminant analysis of principal components (DAPC) was implemented using the R package adegenet (Jombart, Devillard, & Balloux, 2010). The function dapc() was run on the transposed matrix of variance stabilized read counts produced with DESeq2, retaining the number of principal components sufficient to account for 80% of total variance.

2.9.2 | Predicting stress treatment from gene expression

Logistic regression and random forests were used to predict stress treatment based on gene expression. For both classification methods, we divided the data set into a training set including 60% of samples, and a test set including 40% of samples, with stratification by BioProject. Stress treatment for each sample was coded as the outcome variable, with normalized gene counts after controlling for BioProject were used as predictors. Models were trained on the training set, then evaluated based on their performance in predicting stress treatment in the test set. Logistic regression using the lasso method for regularization was performed with the R package glmnet (Friedman, Hastie, & Tibshirani, 2009). The value for lambda was selected based on the lambda.1se value returned by the cv.glmnet function, which is the largest value for lambda such that the cross-validated error was within one standard error of the minimum.

The Random Forest algorithm was also used to predict stress treatment from gene expression. As with logistic regression, predictors were normalized counts for each gene after controlling for BioProject. The algorithm was implemented using the R package randomForest (Liaw & Wiener, 2002). The number of trees grown per iteration (ntree argument) was set to 500, and the number of variables (genes) randomly sampled at each split (mtry argument) was set to 1,000. The performance of both logistic regression and Random Forest models was assessed using confusion matrices built with the R package caret (Kuhn, 2019).

2.9.3 | Weighted gene co-expression network analysis

To identify clusters of coregulated genes associated with stress treatments we used weighted gene co-expression network analysis (WGCNA) (Langfelder & Horvath, 2008). Input for this analysis was the matrix of variance stabilized counts from stress studies after controlling for BioProject using limma. Before network construction, we subset this matrix for the genes that fell within the top 75% for expression level and variance across samples. The goal of this cut-off was to eliminate low-expressed and nonvarying genes that often represent noise, and were unlikely to produce biologically interesting co-expression modules (Langfelder & Horvath, 2017). The resulting subset included 11,284 genes (54.7% of total). We ran WGCNA with a soft threshold power of 12, a minimum module size of 30, and a module merging threshold of 0.3.

2.9.4 | Gene annotations

GO and COG annotations from eggNOG-mapper (Huerta-Cepas et al., 2017, 2019) were included with the reference genome download (Fuller et al., 2019) (Table S5).

2.9.5 | Functional enrichment analysis

Functional enrichment was assessed using two-tailed Mann-Whitney U tests as in Wright, Aglyamova, Meyer, and Matz (2015), using package GO_MWU (https://github.com/z0on/GO_MWU). For differential expression between stress-treated and control corals, we used $-\log_{10}$ transformed raw *p*-values output by DESeq2, multiplied by −1 when the gene was downregulated under stress, as input for the Mann-Whitney U tests (Dixon et al., 2015). The test compares ranks among these transformed *p*-values to assess whether the distribution of ranks of genes included in a GO term diverges significantly from that of all other genes. The deviation of a GO term from the rest of the data set can be quantified by its delta rank (the difference in the mean rank for the GO term and the mean rank for all other genes). Positive delta ranks indicate the GO term tends toward upregulation. Negative values indicate the GO term tends toward downregulation. The similarity of functional responses between data sets was compared by plotting the delta ranks against one another (Figure 4). The tighter the positive relationship between delta ranks, the more similar the GO enrichment is for the differential expression sets being compared. It is important to note that these plots do not represent a formal statistical test, as the data points (gene ontology categories) are not independent since they often encompass overlapping sets of genes, but are a convenient way of observing functional similarity or dissimilarity between differential expression data sets. Functional enrichment for WGCNA modules was tested using Fisher's exact tests on binary calls for module membership.

2.9.6 | Relating WGNA modules to differential expression and GO analyses

As part of our analysis using WGCNA, we related a cluster of coregulated genes, the “red module”, back to previous analyses. One

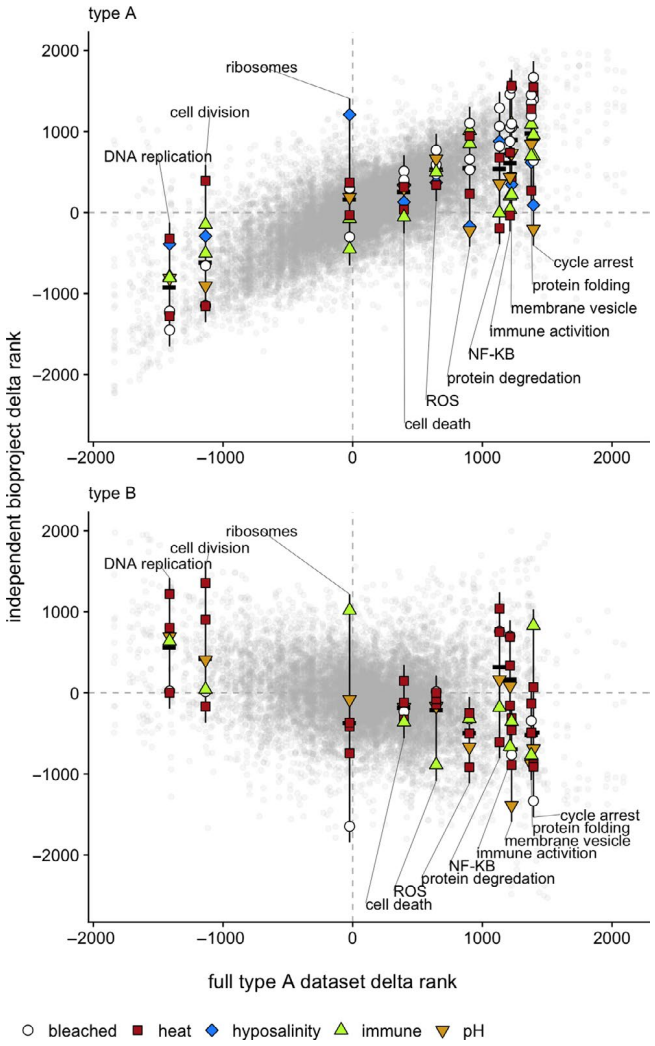

FIGURE 4 Relationships of gene ontology enrichment for individual BioProjects and enrichment when all type A BioProject samples were analysed at once. Delta ranks quantify the tendency of a GO term toward up- or downregulation in stress samples relative to controls. Positive values indicate preferential upregulation under stress treatment. Negative values indicate preferential downregulation. Each panel shows the relationship between delta ranks for individual BioProjects on the Y and those based on all type A samples together on the X. Each grey point represents a single GO term for a single BioProject. Overlaid points connected by vertical lines show BioProjects' mean delta ranks for selected biological processes (Table S6), with colour and shape indicating the type of stress the BioProject used. These processes were selected because they have been previously hypothesized to characterize the coral environmental stress response. Black horizontal dashes indicate the mean delta rank for the selected process across BioProjects. The top panel shows the individual type A BioProjects. The tightness of the relationship here indicates how consistently enrichment in individual BioProjects agreed with overall enrichment based on all type A samples together. The bottom panel shows the individual type B BioProjects. It is important to note that these plots are not intended to show statistical relationships, but are merely a convenient way of comparing functional enrichment across different BioProjects [Colour figure can be viewed at wileyonlinelibrary.com]

simple way to confirm an association identified using WGCNA is to examine the module genes' $\log_2$ fold differences for the same contrast (stress compared to control) from DESeq2. We also used gene module membership to further assess a module's association with Gene Ontology terms. A gene's module membership is the correlation between its expression level across samples and the module's eigengene (Langfelder & Horvath, 2008). It can be thought of as a measure of how much the gene's variation in expression across the samples resembles the module as a whole. By taking the average module membership for all genes in a GO term, we quantified the GO term's similarity in expression to the module as a whole. These mean module membership values were then correlated with delta ranks from the GO_MWU package to assess functional similarity between the module and the differential gene expression results.

3 | RESULTS

To assess whether out methods captured expected gene expression variation, we first summarized the full data set using principal component analysis (PCA). This overview analysis included both studies that applied stress treatments (15 BioProjects) and those that did not (21 BioProjects). After controlling for read counts, PCA revealed clear clustering by BioProject (the study that published the reads) and developmental stage (Figure 1a,b). The first principal component, which accounted for 22% of the variance, correlated with developmental stage, with recruits intermediate to larvae and adults (Figure 1b,c). Hence, across the entire data set, developmental stage was the dominant source of variation in mRNA abundance. For subsequent analyses, we reduced the data set to only those BioProjects that included a stress treatment (see methods).

Counting this study, 15 BioProjects included a stress treatment, with 283 control samples and 335 stressed samples. These encompassed six types of stress: heat, cold, hyposalinity, immune challenge, low pH, and multiple stressors (Figure 2a). Many of the heat, cold, hyposalinity, and multiple samples also experienced bleaching (Figure 2a). Differential expression analysis comparing stress to control samples across this sample set (all stressed versus all controls) detected substantial differential expression, with more than half the genes significant at a false discovery adjusted cutoff of 0.05 (FDR < 0.05) (Figure 2b). After controlling for BioProject, PCA revealed that stress treatment was indeed a dominant source of transcriptional variation (Figure 2c). Discriminant analysis of principal components (DAPC), implemented to discriminate between stressed and control samples, nearly completely separated the stressed and control groups (Figure 2d) and correlated with the first principal component (Figure 2e). Based on the first principal component and discriminant axis, the heat, cold, hyposalinity and multiple treatments tended to produce more severe transcriptomic responses than the pH and immune challenge treatments (Figure 2e). Notably, heat, cold, hyposalinity, and multiple were also the treatments that induced bleaching (Figure 2a).

We next developed classification models of a stressed transcriptome. Using lasso logistic regression and the random forest algorithm, we trained models to predict stress treatment from gene expression data using a training set composed of 60% of the samples randomly sampled with stratification by BioProject. When applied to the withheld set (the remaining 40% of the samples), both models predicted stress treatment with a minimum of 83% accuracy (Figure 2f). In summary, despite differences in species, geography, and the type of stress treatment, shared transcriptomic variation between stress-treated and control samples was detectable among the independent BioProjects.

We next assessed the similarity of stress response between individual projects. Using DESeq2, we computed each gene's $\log_2$ fold change between stress-treated and control samples independently for each of the 14 published studies plus the four experiments from this study. We then correlated these $\log_2$ fold changes between each pair of studies to assess the similarity of transcriptomic responses between them. This comparison revealed a more complex situation than we hypothesized, with two distinct classes of response. Hierarchical clustering based on the correlation of $\log_2$ fold differences revealed that eight published projects, along with the four experiments from this study (88% of all samples), formed a correlated group, with a mean pair-wise Pearson correlation of 0.41 (Figure 3a). If instead of using all genes, we correlated only those that were significant (FDR < 0.05) in the individual studies, the mean correlation increased from 0.41 to 0.67. We refer to this group as the type A response. Notably, the BioProjects in this cluster included all stress types; hence their correlation is consistent with the general stress response paradigm. Surprisingly, however, a second group of six projects formed a distinct cluster that was generally negatively correlated with type A. We refer to this second cluster as the type B response. Correlation of type B BioProjects with each other was weak or nonexistent, with a mean Pearson correlation of 0.045 across all genes (mean = 0.024 for significant genes only).

The contrast between the type A and B responses was further emphasized by repetition of random forest analysis, this time training the model to identify type A stress, type B stress, and controls. Here, type B stress samples were frequently (62% of the time) misidentified as control samples (Figure 3b). While this result is due in part to the smaller sample size for type B, it suggests a lesser distinction between type B stress samples and controls. Consistent with this, type B samples accounted for a large amount of overlap between stressed and control samples on the first principal component and the discriminant axis (Figures 2c–e, 3c, d).

Functional enrichment in type A samples was consistent with the biological processes hypothesized to characterize the coral ESR. Previous studies have consistently linked several biological processes with coral stress, including downregulation of cell division and upregulation of cell death, response to reactive oxygen species, protein degradation, NF-κB signaling, immune response, and protein folding (Aguilar et al., 2019; Barshis et al., 2013; Cziesielski et al., 2018; Cziesielski, Schmidt-Roach, & Aranda, 2019; Table 1). To assess how generally these processes are enriched, we first examined differential expression values for all type A stressed samples compared to all their controls. This analysis identified extensive functional enrichment consistent with the biological processes above (Table S6). We summarize these processes with representative GO terms selected from those most enriched in the type A response (Table S7).

We next examined the enrichment of these processes in each BioProject individually. To illustrate this, we repeated the enrichment analysis independently for each BioProject and compared the results to those obtained from all type A samples together (Figure 4 top panel; Table S6). In particular, response to reactive oxygen species (ROS), and protein folding were enriched for upregulation in all type A BioProjects. One additional process, which we have summarized as membrane vesicle (Table S7) was also universally enriched in type A BioProjects. One exception to our expectations was ribosomes. Across the BioProjects, ribosome biogenesis was sometimes upregulated and sometimes downregulated, with no enrichment for the type A samples as a whole (Figure 4).

Functional enrichment for type B samples was highly distinct from type A. Here, terms linked with cell division tended to be upregulated relative to controls. Although variable, typically hypothesized stress-response processes tended to be downregulated (Figure 4 bottom panel). Similar results were found when comparing enrichment from individual BioProjects to that of all type B samples together (Figure S7).

A general stress response could be described in terms of a group of coregulated genes that responds similarly to all types of stress. With this in mind, we used weighted gene co-expression network snalysis (WGCNA) to identify clusters (referred to as modules) of co-regulated genes and examined their association with stress treatments. The full WGCNA dendrogram and correlation heatmap are shown in (Figure S8). The three largest modules are shown in Figure 5. The red module appeared to capture the type A stress response. This module was upregulated for all types of stress in type A BioProjects and enriched with gene ontology categories indicative of transcription factors, cell death, proteolysis, and growth inhibition (Figure 5; Table S8). The much larger green module, essentially capturing the background of the transcriptome (Figure S8), was downregulated by all types of stress among type A BioProjects. The green module was functionally enriched with genes associated with growth and metabolism (Figure 5; Table S8). Notably, we did not detect any modules consistent for the type B response (Figure S8). Regarding red and green modules, type B samples tended to be regulated in the opposite direction of type A. This is consistent with our other results (Figures 3a, 4b).

Expression of the white module was varied across stress types, upregulated by bleaching, heat, and hyposalinity, but downregulated by immune challenge and pH. Downregulation under immune challenge was especially surprising, as the module was enriched for genes associated with immune response as well as membrane vesicles and transporters (Figure 5; Table S8). The treatment associations and functional enrichment for this module suggest it may capture elements of the bleaching response.

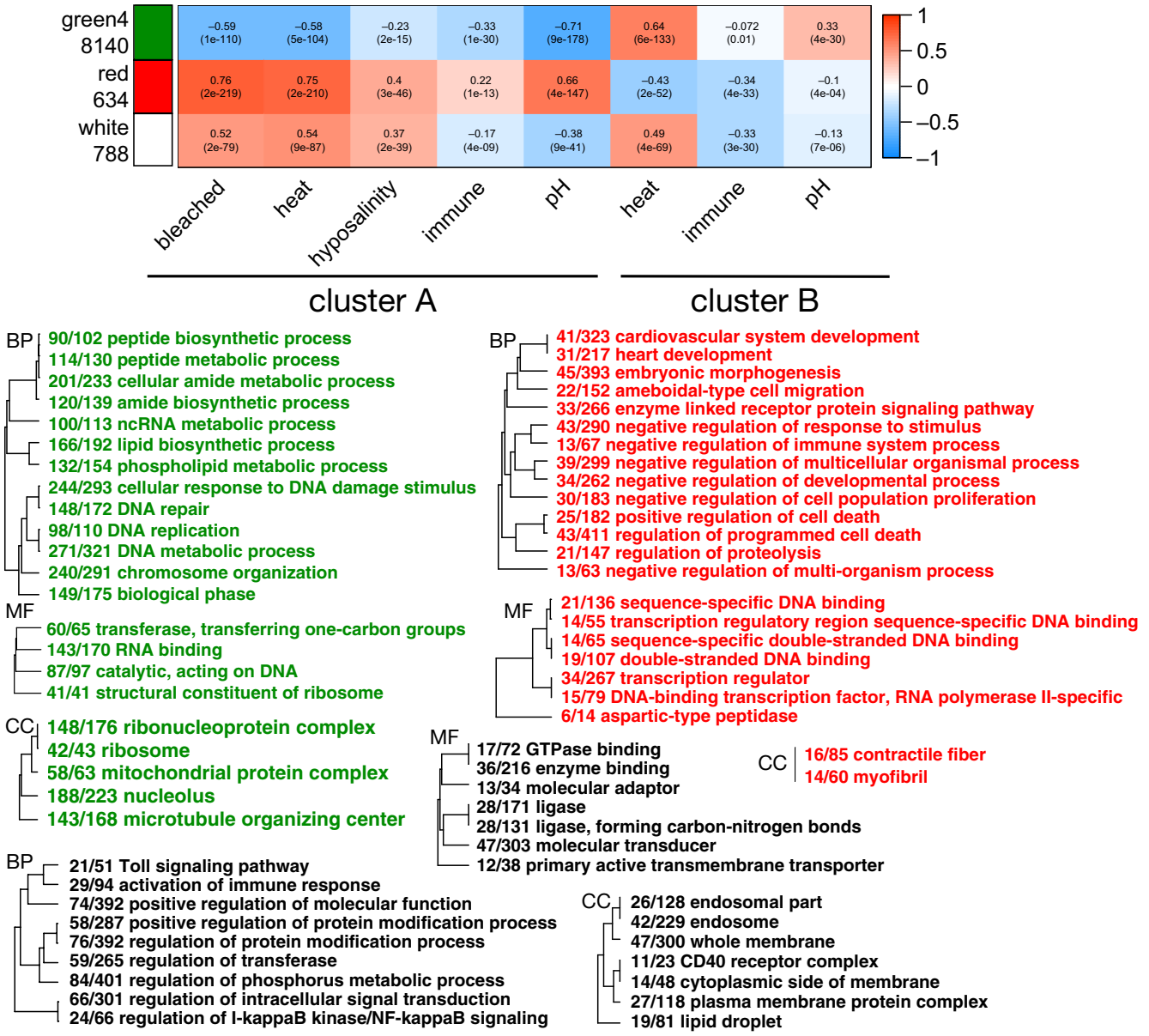

FIGURE 5 Module-trait correlations and gene ontology enrichment for three largest WGCNA modules. The heatmap illustrates correlations between the modules and stress treatments. The colour scale indicates Pearson correlation. The number beneath each module title indicates the number of genes assigned to it. For correlation with stress treatments, samples were divided based on the clusters shown in Figure 3 (type A and type B). Colour coded dendrograms show top enriched gene ontology terms for each module. All terms were enriched with a maximum FDR-adjusted *p*-value of 0.05 (Fisher's exact test) [Colour figure can be viewed at wileyonlinelibrary.com]

As the red module (identified in an unsupervised manner, solely from patterns of gene expression correlations) appeared associated with a general stress response, we examined its correspondence with previous results. First, we confirm that genes in the red module were consistently upregulated in response to stress treatment among type A BioProjects (Figure 6a). Indeed, division between the type A and type B BioProjects was largely predicted by whether or not the module was upregulated in stress-treated samples. Consistent with this division, higher expression of the red module in stress-treated samples predicted stronger correlations within the type A cluster (Figures 3a, 6b). Additionally, GO terms' mean membership in the red module were similar to GO enrichment patterns observed for the type A stress response shown in Figure 4a (Figure 6c). In other words, the more a GO term's expression correlated with the red module, the more enriched that GO term was for upregulation in the type A stress response. In summary, the red module efficiently recapitulated aspects of the general stress response identified by previous analyses based on the entire transcriptome.

4 | DISCUSSION

In this study, we analysed previously published and newly generated Tag-seq and RNA-seq data to assess the hypothesis of a general stress

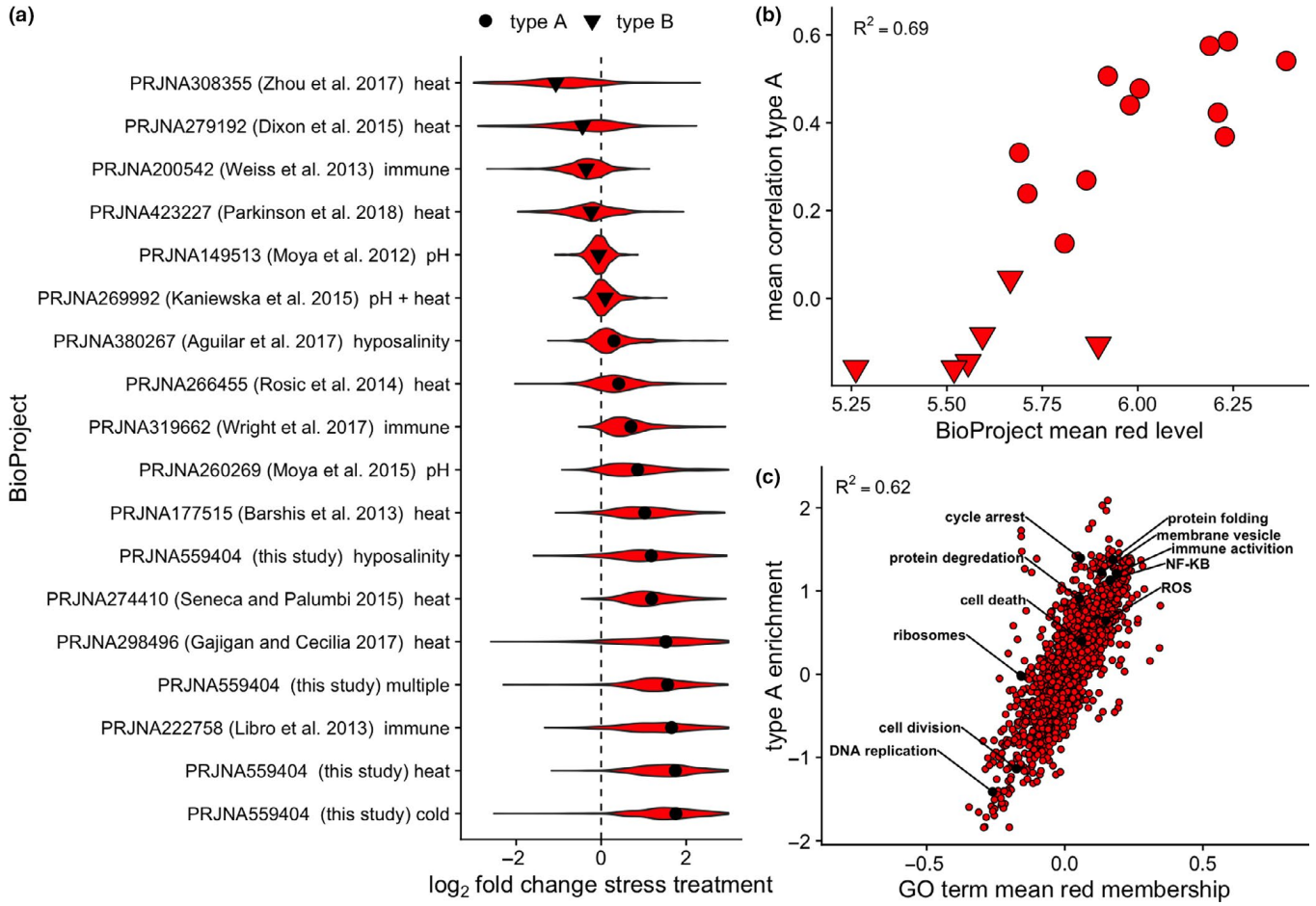

FIGURE 6 Comparing the red module with previous analyses. (a) Distribution of each BioProject's $\log_2$ fold changes in response to stress for red module genes. Points at the center of each violin indicate the median. Point shape indicates whether the BioProject clustered with the type A response or type B response in Figure 3a. Y axis labels show the BioProject accession, study reference, and the type of stress treatment applied. (b) Scatterplot of mean red module expression levels in stress treated samples from each BioProject against the BioProject's mean Pearson correlation with the type A cluster (Figure 3a). Point shape indicates type A and type B BioProjects as in (a). (c) Scatterplot of GO term's mean red module membership against the delta rank for all type A samples from Figure 4 [Colour figure can be viewed at wileyonlinelibrary.com]

response in the genus *Acropora*. Contrary to expectations, we detected not one, but two classes of responses. The first of these, represented by type A in Figure 3, was consistent with a general coral environmental stress response (ESR). Responses among these BioProjects tended to be correlated, and functionally enriched for previously hypothesized biological processes. Specifically, we detected significant upregulation for genes involved in cell death, response to reactive oxygen species, NF-κB signaling, immune response, protein folding, and protein degradation. Surprisingly, the second cluster captured an entirely distinct transcriptional response, negatively related to type A.

WGCNA further supported these results. A module of 634 co-regulated genes and a contrasting module of over 8,000 genes were up- and downregulated by all types of stress for type A respectively, but tended to be oppositely regulated in type B. The consistently opposing expression patterns of the red and green modules (Figure 5) suggest their regulation may be mechanistically linked. Enrichment of GO terms involved in cell division and metabolism in the green module and negative regulation of growth and development in the red module suggests this mechanistic link may be inherent to modules themselves. Based on this, we propose that the negative relationship between these modules is a programmed aspect of the coral ESR. Tracking the expression of these modules through time as a stress response is mounted could elucidate this link in more subtle mechanistic detail. A third module, enriched for immune, vesicle, and transport genes, was associated only with stressors that induced bleaching. As this module was not induced by immune challenge (Figure 5), the enriched immune GO classes may involve interactions with algal symbionts.

The primary difference between the two response types appeared to be the severity of the stress. First, the median absolute $\log_2$ fold change (across all genes) between stress and control samples for type A (0.297) was greater than type B (0.222), (approximately 5% greater on a linear scale; t test $p < 1e{-}9$). Median $\log_2$ fold changes for individual BioProjects from 0.161 to 0.706 for type A and from 0.123 to 0.428 for type B. For individual BioProjects, median $\log_2$ differences ranged from 0.161 to 0.706 for type A and from 0.123 to 0.428 for type B. This heightened response is suggestive of

more severe stress in type A. This difference was further supported by the distribution of the stressed samples along the first principal component and the discriminant axis (Figure 3b, c). As these two axes largely captured transcriptomic variation between control and stressed corals, the tendency of type B samples toward their centers indicates less severe transcriptomic response. The frequency of bleaching was also much higher for type A (Figure 3a). Indeed, only one study in cluster B reported bleaching, and this was described as "mild coral bleaching" (Kaniewska et al., 2015). Higher induction of bleaching matched with the generally higher temperatures used for heat treatment (median = 34°C across type A BioProjects; median = 32°C for type B) (Table S1). One exception was Parkinson et al. (2018; PRJNA423227), who used heat treatments of 35°C. As treatment duration in this study was only 1 hr (Table S1), there may not have been sufficient time to mount the general response observed in type A. Among the three BioProjects that applied immune challenges, the two in type A applied more severe stresses. Libro, Kaluziak, and Vollmer (2013; PRJNA222758) sampled tissue that was at or adjacent to visible interfaces of white band disease, and Wright et al. (2017; PRJNA319662) physically abraded half their samples, and observed severe, albeit varied, mortality in the immune challenged group. In type B on the other hand, Weiss et al. (2013; PRJNA200542) injected their samples with immunogens (muramyl dipeptide and polyinosinic:polycytidylic acid), which were intended to elicit a specific immune response by mimicking infectious agents. In general, pH appeared to elicit less severe expression changes than other treatments. Indeed, reports of the physiological severity of elevated pCO_2 on corals are varied (Langdon & Atkinson, 2005; Rodolfo-Metalpa, Martin, Ferrier-Pagès, & Gattuso, 2010), and corals may very well be capable of resilience (McCulloch, Falter, Trotter, & Montagna, 2012). The only study using pH treatment to show the type A response was Moya et al. (2014; PRJNA260269), whereas a similar experiment by the same group (Moya et al., 2012; PRJNA149513) was type B. The difference here was a prolonged exposure (nine days beginning immediately post-fertilization in Moya et al. (2014) rather than short term (three days beginning immediately after settlement in Moya et al., 2012; Table S1).

To summarize, the main difference between the two stress types appeared to be severity of the stress induced, with higher stress in type A. This is consistent with the proposed role of the yeast ESR, to serve as a blanket response that prepares cells to protect themselves under diverse types of stress (Gasch, 2003; Gasch et al., 2000). The relatively weak correlations observed within type B may instead reflect specific transcriptional responses to different stressful conditions that did not reach levels sufficient to induce the general coral ESR. Hence contrary to our expectations, the severity of a stress treatment may not only affect the magnitude of transcriptional response but its functional nature.

The surprising negative relationship between the two response types may explain previous inconsistencies between gene expression studies. For instance, Barshis et al. (2013) hypothesized that corals adapt to stressful conditions by constitutively expressing stress response genes at higher levels (transcriptional "frontloading"). According to this hypothesis, constitutive profiles more similar to stressed individuals should produce higher tolerance. Contrary to this hypothesis, Dixon et al. (2015) found that larval cultures with greater transcriptomic similarity to heat-stressed adults had lower heat tolerance. Here we find that the adult heat treatment from Dixon et al. (2015)(31.5°C for 72 hr) fell into the type B response, weakly opposite the type A response observed for Barshis et al. (2013). In other words, if Dixon et al. (2015) had stressed their adult corals more severely, their results may have supported "frontloading" sensu Barshis et al. (2013). We hope that delineation of the coral ESR presented here will assist in addressing similar questions in future studies. For instance, the mean expression level of the red module, or one or more of its hub genes, could be used as a simple benchmark for the degree of ESR activation in an RNA-seq profile. Coupling such a summary statistic with physiological data could help determine how baseline ESR and ESR plasticity contributes to coral resilience.

Gene annotation is a major challenge in ecological genomics. For instance, with this data set, we identified a final set of 25 genes that were members of the red module and upregulated for every type A BioProject with a minimum fold change of 1.5 ($\log_2$ fold change > 0.59) (Table S9). Among the annotated genes in this set were two were heat shock proteins, two oxidase/oxidoreductases, two involving retro-transposition, a TNF receptor-associated factor, a matrix metallopeptidase, and a transcription factor. However, 13 of these genes (52%) lacked annotations. Given the diversity of studies included, these unknown genes can be confidently labeled as stress response genes. Based on our results we have generated similar contextual annotations for *A. millepora* genes including bleaching ($|\log_2$ fold change$|$> 0.59 in all type A bleached BioProjects) and two tiers of general stress response (the core set described above and a more lenient set with $|\log_2$ fold change$|$ > 0.32 in > 80% of type A BioProjects) (Table S9). The differential expression results for all type A, all type B, and each individual BioProject are available in Table S10. We hope that this first effort will improve in scope and detail with the addition of more gene expression studies in the future.

ACKNOWLEDGEMENTS

This study was supported by the National Science Foundation grant IOS-1755277 to M.V.M. Data analysis was performed with the help of the Texas Advanced Computing Centre.

AUTHOR CONTRIBUTIONS

G.D., designed and performed the research, analysed the data, and wrote the paper. E.A., performed the research, and analysed the data. M.M. performed the research, and wrote the paper.

DATA AVAILABILITY STATEMENT

Reads generated for this study have been uploaded to the SRA database project accession PRJNA559404. All scripts for data processing and analysis, as well as intermediate datasets are available on Github: https://github.com/grovesdixon/Acropora_gene_expression_meta

ORCID

Groves Dixon https://orcid.org/0000-0001-5501-6024

REFERENCES

Abdulla, E. M., & Campbell, I. C. (1996). Studies of neurotoxicity in cellular models. In I. J. V. Castell, & M. J. Gómez-Lechón (Eds.), *In Vitro methods in pharmaceutical research* (pp. 155–180). https://doi.org/10.1016/B978-0-12-163390-5.50021-1

Aguilar, C., Raina, J. B., Fôret, S., Hayward, D. C., Lapeyre, B., Bourne, D. G., & Miller, D. J. (2019). Transcriptomic analysis reveals protein homeostasis breakdown in the coral *Acropora millepora* during hypo-saline stress 06 Biological Sciences 0604 Genetics. *BMC Genomics*, *20*(1), 1–13. https://doi.org/10.1186/s12864-019-5527-2

Aguilar, C., Raina, J. B., Motti, C. A., Fôret, S., Hayward, D. C., Lapeyre, B., … Miller, D. J. (2017). Transcriptomic analysis of the response of Acropora millepora to hypo-osmotic stress provides insights into DMSP biosynthesis by corals. *BMC Genomics*, *18*(1). http://dx.doi.org/10.1186/s12864-017-3959-0

Andrews, S. (2010). FASTQC: A quality control tool for high throughput sequence data.

Barshis, D. J., Ladner, J. T., Oliver, T. A., Seneca, F. O., Traylor-Knowles, N., & Palumbi, S. R. (2013). Genomic basis for coral resilience to climate change. *Proceedings of the National Academy of Sciences of USA*, *110*(4), 1387–1392. https://doi.org/10.1073/pnas.1210224110

Bay, R. A., Rose, N. H., Logan, C. A., Palumbi, S. R. (2017). Genomic models predict successful coral adaptation if future ocean warming rates are reduced. *Science Advances*, *3*(11), e1701413. http://dx.doi.org/10.1126/sciadv.1701413

Bertucci, A., Forêt, S., Ball, E. E., Miller, D. J. (2015). Transcriptomic differences between day and night inAcropora milleporaprovide new insights into metabolite exchange and light-enhanced calcification in corals. *Molecular Ecology*, *24*(17), 4489–4504. http://dx.doi.org/10.1111/mec.13328

Brion, C., Pflieger, D., Souali-Crespo, S., Friedrich, A., & Schacherer, J. (2016). Differences in environmental stress response among yeasts is consistent with species-specific lifestyles. *Molecular Biology of the Cell*, *27*(10), 1694–1705. https://doi.org/10.1091/mbc.e15-12-0816

Cziesielski, M. J., Liew, Y. J., Cui, G., Schmidt-Roach, S., Campana, S., Marondedze, C., & Aranda, M. (2018). Multi-omics analysis of thermal stress response in a zooxanthellate cnidarian reveals the importance of associating with thermotolerant symbionts. *Proceedings of the Royal Society B: Biological Sciences*, *285*(1877). https://doi.org/10.1098/rspb.2017.2654

Cziesielski, M. J., Schmidt-Roach, S., & Aranda, M. (2019). The past, present, and future of coral heat stress studies. *Ecology and Evolution*, *17*, 10055–10066. https://doi.org/10.1002/ece3.5576

DeSalvo, M. K., Estrada, A., Sunagawa, S., & Medina, M. (2012). Transcriptomic responses to darkness stress point to common coral bleaching mechanisms. *Coral Reefs*, *31*(1), 215–228. https://doi.org/10.1007/s00338-011-0833-4

Dixon, G., Bay, L. K., & Matz, M. V. (2014). Bimodal signatures of germline methylation are linked with gene expression plasticity in the coral *Acropora millepora*. *BMC Genomics*, *15*, 1109. https://doi.org/10.1186/1471-2164-15-1109

Dixon, G., Bay, L. K., & Matz, M. V. (2016). Evolutionary consequences of DNA methylation in a basal metazoan. *Molecular Biology and Evolution*, *33*(9), 2285–2293. https://doi.org/10.1101/043026

Dixon, G. B., Davies, S. W., Aglyamova, G. V., Meyer, E., Bay, L. K., & Matz, M. V. (2015). Genomic determinants of coral heat tolerance across latitudes. *Science*, *348*(6242), 1460–1462.

Drury, C. (2019). Resilience in reef-building corals: The ecological and evolutionary importance of the host response to thermal stress. *Molecular Ecology*, *29*, 448–465. https://doi.org/10.1017/CBO9781107415324.004

Friedman, J., Hastie, T., & Tibshirani, R. (2009). Regularization paths for generalized linear models via coordinate descent. *Journal of Statistical Software*, *33*(1), 128–129. https://doi.org/10.1002/wics.10

Fuller, Z. L., Mocellin, V. J. L., Morris, L., Cantin, N., Sarre, L., Peng, J., … Przeworski, M. (2019). Population genetics of the coral *Acropora millepora*: Towards a genomic predictor of bleaching. *BioRxiv* Pre-Print. https://doi.org/10.1101/867754

Gajigan, A. P., & Conaco, C. (2017). A microRNA regulates the response of corals to thermal stress. *Molecular Ecology*, *26*(13), 3472–3483. http://dx.doi.org/10.1111/mec.14130

Gasch, A. P. (2003).The environmental stress response: a common yeast response to diverse environmental stresses. In S. Hohmann, & W. H. Mager (Eds.), *Yeast stress responses*, Vol. *1* (pp. 11–70). https://doi.org/10.1007/3-540-45611-2_2

Gasch, A. P., Spellman, P. T., Kao, C. M., Carmel-Harel, O., Eisen, M. B., Storz, G., … Brown, P. O. (2000). Genomic expression programs in the response of yeast cells to environmental changes. *Molecular Biology of the Cell*, *11*(12), 4241–4257. https://doi.org/10.1091/mbc.11.12.4241

Hammond, E. M., & Giaccia, A. J. (2005). The role of p53 in hypoxia-induced apoptosis. *Biochemical and Biophysical Research Communications*, *331*(3), 718–725. https://doi.org/10.1016/j.bbrc.2005.03.154

Huerta-Cepas, J., Forslund, K., Coelho, L. P., Szklarczyk, D., Jensen, L. J., Von Mering, C., & Bork, P. (2017). Fast genome-wide functional annotation through orthology assignment by eggNOG-mapper. *Molecular Biology and Evolution*, *34*(8), 2115–2122. https://doi.org/10.1093/molbev/msx148

Huerta-Cepas, J., Szklarczyk, D., Heller, D., Hernández-Plaza, A., Forslund, S. K., Cook, H., … Bork, P. (2019). EggNOG 5.0: A hierarchical, functionally and phylogenetically annotated orthology resource based on 5090 organisms and 2502 viruses. *Nucleic Acids Research*, *47*(D1), D309–D314. https://doi.org/10.1093/nar/gky1085

Jombart, T., Devillard, S., & Balloux, F. (2010). Discriminant analysis of principal components: A new method for the analysis of genetically structured populations. *BMC Genetics*, *11*(1), 94. https://doi.org/10.1186/1471-2156-11-94

Kaniewska, P., Alon, S., Karako-Lampert, S., Hoegh-Guldberg, O., & Levy, O. (2015). Signaling cascades and the importance of moonlight in coral broadcast mass spawning. *eLife*, *4*, http://dx.doi.org/10.7554/elife.09991

Kaniewska, P., Chan, C.-K., Kline, D., Ling, E. Y. S., Rosic, N., Edwards, D., … Dove, S. (2015). Transcriptomic changes in coral holobionts provide insights into physiological challenges of future climate and ocean change. *PLoS One*, *10*(10), 1–30. https://doi.org/10.1371/journal.pone.0139223

Kenkel, C. D., & Matz, M. V. (2016). Enhanced gene expression plasticity as a mechanism of adaptation to a variable environment in a reef-building coral. *Nature Ecology & Evolution*, *1*, 0014. https://doi.org/10.1101/059667

Kenkel, C. D., Meyer, E., & Matz, M. V. (2013). Gene expression under chronic heat stress in populations of the mustard hill coral (*Porites astreoides*) from different thermal environments. *Molecular Ecology*, *22*(16), 4322–4334. https://doi.org/10.1111/mec.12390

Kenkel, C. D., Moya, A., Strahl, J., Humphrey, C., & Bay, L. K. (2018). Functional genomic analysis of corals from natural CO 2 -seeps reveals core molecular responses involved in acclimatization to ocean acidification. *Global Change Biology*, *24*(1), 158–171. https://doi.org/10.1111/gcb.13833

Kuhn, M. (2019). caret. Classification and Regression Training.

Langdon, C., & Atkinson, M. J. (2005). Effect of elevated pCO2 on photosynthesis and calcification of corals and interactions with seasonal change in temperature/ irradiance and nutrient enrichment. *Journal of Geophysical Research C: Oceans*, *110*(9), 1–16. https://doi.org/10.1029/2004JC002576

Langfelder, P., & Horvath, S. (2008). WGCNA: An R package for weighted correlation network analysis. *BMC Bioinformatics*, *9*, 559. https://doi.org/10.1186/1471-2105-9-559

Langfelder, P., & Horvath, S. (2017). WGCNA package FAQ. Retrieved from https://horvath.genetics.ucla.edu/html/CoexpressionNetwork/Rpackages/WGCNA/faq.html

Langmead, B., & Salzberg, S. L. (2012). Fast gapped-read alignment with BOWTIE 2. *Nature Methods*, *9*(4), 357–359. https://doi.org/10.1038/nmeth.1923

Li, H., Handsaker, B., Wysoker, A., Fennell, T., Ruan, J., Homer, N., … Durbin, R. (2009). The Sequence Alignment/Map format and SAMtools. *Bioinformatics*, *25*(16), 2078–2079. https://doi.org/10.1093/bioinformatics/btp352

Liao, Y., Smyth, G. K., & Shi, W. (2014). FEATURECOUNTS: An efficient general purpose program for assigning sequence reads to genomic features. *Bioinformatics*, *30*(7), 923–930. https://doi.org/10.1093/bioinformatics/btt656

Liaw, A., & Wiener, M. (2002). Classification and Regression by randomForest. *R News*, *2*(3), 18–22.

Libro, S., Kaluziak, S. T., & Vollmer, S. V. (2013). RNA-seq profiles of immune related genes in the staghorn coral *Acropora cervicornis* Infected with white band disease. *PLoS One*, *8*(11), 1–11. https://doi.org/10.1371/journal.pone.0081821

Love, M. I., Huber, W., & Anders, S. (2014). Moderated estimation of fold change and dispersion for RNA-Seq data with DESeq2. *Genome Biology*, *15*(550), 1–21. https://doi.org/10.1101/002832

Maor-Landaw, K., Karako-Lampert, S., Ben-Asher, H. W., Goffredo, S., Falini, G., Dubinsky, Z., & Levy, O. (2014). Gene expression profiles during short-term heat stress in the red sea coral *Stylophora pistillata*. *Global Change Biology*, *20*, 3026–3035. https://doi.org/10.1111/gcb.12592

Martin, M. (2011). Cutadapt removes adapter sequences from high-throughput sequencing reads. *Embnetjournal*, *17*(1), 10–12. https://doi.org/10.14806/ej.17.1.200

McCulloch, M., Falter, J., Trotter, J., & Montagna, P. (2012). Coral resilience to ocean acidification and global warming through pH up-regulation. *Nature Climate Change*, *2*(8), 623–627. https://doi.org/10.1038/nclimate1473

Meyer, E., Aglyamova, G. V., & Matz, M. V. (2011). Profiling gene expression responses of coral larvae (*Acropora millepora*) to elevated temperature and settlement inducers using a novel RNA-Seq procedure. *Molecular Ecology*, *20*(17), 3599–3616. https://doi.org/10.1111/j.1365-294X.2011.05205.x

Mohamed, A. R., Cumbo, V., Harii, S., Shinzato, C., Chan, C. X., Ragan, M. A., … Miller, D. J. (2016). The transcriptomic response of the coralAcropora digitiferato a competentSymbiodiniumstrain: the symbiosome as an arrested early phagosome. *Molecular Ecology*, *25*(13), 3127–3141. http://dx.doi.org/10.1111/mec.13659

Mohamed, A. R., Cumbo, V. R., Harii, S., Shinzato, C., Chan, C. X., … Miller, D. J. (2018). Deciphering the nature of the coral–Chromera association. *The ISME Journal*, *12*(3), 776–790. http://dx.doi.org/10.1038/s41396-017-0005-9

Moya, A., Huisman, L., Ball, E. E., Hayward, D. C., Grasso, L. C., Chua, C. M., … Miller, D. J. (2012). Whole transcriptome analysis of the coral *Acropora millepora* reveals complex responses to CO_2-driven acidification during the initiation of calcification. *Molecular Ecology*, *21*(10), 2440–2454. https://doi.org/10.1111/j.1365-294X.2012.05554.x

Moya, A., Huisman, L., Forêt, S., Gattuso, J.-P., Hayward, D. C., Ball, E. E., & Miller, D. J. (2015). Rapid acclimation of juvenile corals to CO2-mediated acidification by upregulation of heat shock protein and Bcl-2 genes. *Molecular Ecology*, *24*(2), 438–452. http://dx.doi.org/10.1111/mec.13021

Moya, A., Huisman, L., Forêt, S., Gattuso, J. P., Hayward, D. C., Ball, E. E., & Miller, D. J. (2014). Rapid acclimation of juvenile corals to CO2-mediated acidification by upregulation of heat shock protein and Bcl-2 genes. *Molecular Ecology*, *24*(2), 438–452. https://doi.org/10.1111/mec.13021

Oldach, M. J., & Vize, P. D. (2018). De novo assembly and annotation of the Acropora gemmifera transcriptome. *Marine Genomics*, *40*, 9–12. http://dx.doi.org/10.1016/j.margen.2017.12.007

Palumbi, S. R., Barshis, D. J., Traylor-Knowles, N., Bay, R. A. (2014). Mechanisms of reef coral resistance to future climate change. *Science*, *344*(6186), 895–898. http://dx.doi.org/10.1126/science.1251336

Parkinson, J. E., Bartels, E., Devlin-Durante, M. K., Lustic, C., Nedimyer, K., Schopmeyer, S., … Baums, I. B. (2018). Extensive transcriptional variation poses a challenge to thermal stress biomarker development for endangered corals. *Molecular Ecology*, *27*(5), 1103–1119. https://doi.org/10.1111/mec.14517

Reyes-Bermudez, A., Villar-Briones, A., Ramirez-Portilla, C., Hidaka, M., Mikheyev, A. S. (2016). Developmental progression in the coral acropora digitiferals controlled by differential expression of distinct regulatory gene networks. *Genome Biology and Evolution*, *8*(3), 851–870. http://dx.doi.org/10.1093/gbe/evw042

Ritchie, M. E., Phipson, B., Wu, D., Hu, Y., Law, C. W., Shi, W., & Smyth, G. K. (2015). limma powers differential expression analyses for RNA-sequencing and microarray studies. *Nucleic Acids Research*, *43*(7), e47. https://doi.org/10.1093/nar/gkv007

Rocker, M. M., Kenkel, C. D., Francis, D. S., Willis, B. L., & Bay, L. K. (2019). Plasticity in gene expression and fatty acid profiles of Acropora tenuis reciprocally transplanted between two water quality regimes in the central Great Barrier Reef, Australia. *Journal of Experimental Marine Biology and Ecology*, *511*, 40–53. http://dx.doi.org/10.1016/j.jembe.2018.11.004

Rodolfo-Metalpa, R., Martin, S., Ferrier-Pagès, C., & Gattuso, J.-P. (2010). Response of the temperate coral Cladocora caespitosa to mid- and long-term exposure to pCO2 and temperature levels projected for the year 2100 AD. *Biogeosciences*, *7*, 289–300. https://doi.org/10.5194/bg-7-289-2010

Ron, E. Z. (2006). Bacterial Stress Response. In M. Dworkin, S. Falkow, & E. Rosenberg (Eds.), *The Prokaryotes A Handbook on the Biology of Bacteria Volume 2: Ecophysiology and Biochemistry* (3rd edn., pp. 1012–1027). https://doi.org/10.1007/0-387-30742-7_32

Rose, N. H., Bay, R. A., Morikawa, M. K., & Palumbi, S. R. (2018). Polygenic evolution drives species divergence and climate adaptation in corals. *Evolution*, *72*(1), 82–94. http://dx.doi.org/10.1111/evo.13385

Rosenberg, Y., Doniger, T., Harii, S., Sinniger, F., & Levy, O. (2017). Canonical and cellular pathways timing gamete release inAcropora digitifera,Okinawa, Japan. *Molecular Ecology*, *26*(10), 2698–2710. http://dx.doi.org/10.1111/mec.14062

Rosic, N., Kaniewska, P., Chan, C. K., Ling, E. Y., Edwards, D., Dove, S., & Hoegh-Guldberg, O. (2014). Early transcriptional changes in the reef-building coral Acropora aspera in response to thermal and nutrient stress. *BMC Genomics*, *15*(1), 1052. http://dx.doi.org/10.1186/1471-2164-15-1052

Ruiz-Jones, L. J., & Palumbi, S. R. (2017). Tidal heat pulses on a reef trigger a fine-tuned transcriptional response in corals to maintain homeostasis. *Science Advances*, *3*(3), e1601298. http://dx.doi.org/10.1126/sciadv.1601298

Seneca, F. O., & Palumbi, S. R. (2015). The role of transcriptome resilience in resistance of corals to bleaching. *Molecular Ecology*, *24*(7), 1467–1484. http://dx.doi.org/10.1111/mec.13125

Strader, M. E., Aglyamova, G. V., & Matz, M. V. (2016). Red fluorescence in coral larvae is associated with a diapause-like state. *Molecular Ecology*, *25*(2), 559–569. http://dx.doi.org/10.1111/mec.13488

Strader, M. E., Aglyamova, G. V., & Matz, M. V. (2018). Molecular characterization of larval development from fertilization to metamorphosis in a reef-building coral. *BMC Genomics*, *19*(1). http://dx.doi.org/10.1186/s12864-017-4392-0

Takahashi-Kariyazono, S., Gojobori, J., Satta, Y., Sakai, K., & Terai, Y. (2016). Acropora digitifera encodes the largest known family of fluorescent proteins that has persisted during the evolution of acropora

species. *Genome Biology and Evolution*, *8*(11), 3271–3283. http://dx.doi.org/10.1093/gbe/evw265

Takahashi-Kariyazono, S., Sakai, K., & Terai, Y. (2018). Presence–absence polymorphisms of highly expressed FP sequences contribute to fluorescent polymorphisms in acropora digitifera. *Genome Biology and Evolution*, *10*(7), 1715–1729. http://dx.doi.org/10.1093/gbe/evy122

Weber, H., Polen, T., Heuveling, J., Wendisch, V. F., Hengge, R., Ju, F., & Al, W. E. T. (2005). Genome-wide analysis of the general stress response network in *Escherichia coli*: Sigma S-dependent genes, promoters, and sigma factor selectivity. *Journal of Bacteriology*, *187*(5), 1591–1603. https://doi.org/10.1128/JB.187.5.1591

Weiss, Y., Forêt, S., Hayward, D. C., Ainsworth, T., King, R., Ball, E. E., & Miller, D. J. (2013). The acute transcriptional response of the coral *Acropora millepora* to immune challenge: Expression of GiMAP/IAN genes links the innate immune responses of corals with those of mammals and plants. *BMC Genomics*, *14*(400). https://doi.org/10.1186/1471-2164-14-400

Wright, R. M., Aglyamova, G. V., Meyer, E., & Matz, M. V. (2015). Gene expression associated with white syndromes in a reef building coral, *Acropora hyacinthus*. *BMC Genomics*, *16*(1), 371. https://doi.org/10.1186/s12864-015-1540-2

Wright, R. M., Kenkel, C. D., Dunn, C. E., Shilling, E. N., Bay, L. K., & Matz, M. V. (2017). Intraspecific differences in molecular stress responses and coral pathobiome contribute to mortality under bacterial challenge in *Acropora millepora*. *Scientific Reports*, *7*(1), 1–13. https://doi.org/10.1038/s41598-017-02685-1

Yasuoka, Y., Shinzato, C., & Satoh, N. (2016). The mesoderm-forming gene brachyury regulates ectoderm-endoderm demarcation in the coral acropora digitifera. *Current Biology*, *26*(21), 2885–2892. http://dx.doi.org/10.1016/j.cub.2016.08.011

Young, J. W., Locke, J. C. W., & Elowitz, M. B. (2013). Rate of environmental change determines stress response specificity. *Proceedings of the National Academy of Sciences*, *110*(10), 4140–4145. https://doi.org/10.1073/pnas.1213060110

Yuan, X., Yuan, T., Huang, H., Jiang, L., Zhou, W., & Liu, S. (2018). Elevated CO2 delays the early development of scleractinian coral Acropora gemmifera. *Scientific Reports*, *8*(1). http://dx.doi.org/10.1038/s41598-018-21267-3

Zhou, Z., Wu, Y., Zhang, C., Li, C., Chen, G., Yu, X., … Huang, B. (2017). Suppression of NF-κB signal pathway by NLRC3-like protein in stony coral Acropora aculeus under heat stress. *Fish & Shellfish Immunology*, *67*, 322–330. http://dx.doi.org/10.1016/j.fsi.2017.06.027

SUPPORTING INFORMATION

Additional supporting information may be found online in the Supporting Information section.

How to cite this article: Dixon G, Abbott E, Matz M. Meta-analysis of the coral environmental stress response: *Acropora* corals show opposing responses depending on stress intensity. *Mol Ecol*. 2020;29:2855–2870. https://doi.org/10.1111/mec.15535